Determination of the ^{64}Zn,^{47}Ti(n,p) Cross-Sections using a DD Neutron Generator for Medical Isotope Studies

A.S. Voyles[a,*], M.S. Basunia[b], J.C. Batchelder[b], J.D. Bauer[c], L.A. Bernstein[a,b], E.F. Matthews[a], D. Rutte[d,e], M.A. Unzueta[a], K.A. van Bibber[a]

[a]*Department of Nuclear Engineering, University of California, Berkeley, Berkeley CA, 94720 USA*
[b]*Lawrence Berkeley National Laboratory, Berkeley CA, 94720 USA*
[c]*Lawrence Livermore National Laboratory, Livermore CA, 94551 USA*
[d]*Berkeley Geochronology Center, Berkeley CA, 94709 USA*
[e]*Department of Earth and Planetary Sciences, University of California, Berkeley, Berkeley CA, 94720 USA*

Abstract

Cross sections for the ^{47}Ti(n,p)^{47}Sc and ^{64}Zn(n,p)^{64}Cu reactions have been measured for quasi-monoenergetic DD neutrons produced by the UC-Berkeley High Flux Neutron Generator. The study was motivated by interest in the production of ^{47}Sc and ^{64}Cu as emerging medical isotopes. The cross sections were measured in ratio to the ^{113}In(n,n')^{113m}In and ^{115}In(n,n')^{115m}In inelastic scattering reactions on co-irradiated indium samples. Post-irradiation counting using an HPGe and LEPS detectors allowed for cross section determination to within 6% uncertainty. The cross section were determined with lower uncertainty than existing measurements and are found to be in good agreement with the literature and theoretical values. This work highlights the utility of using DD plasma-based neutron sources, for a host of nuclear data measurements and potentially for the production of radionuclides for medical applications.

> ASV: The abstract is now nicely short and sweet, but should it be expanded at all?

> ASV: For my corresponding author email, should I list my Gmail (more permanent) or my Berkeley / LBL address (more professional)?

*Corresponding author
Email address:* andrew.voyles@gmail.com (A.S. Voyles)

1. Introduction

There has been significant interest in the past several years in exploring the use of neutron-induced reactions to create radionuclides for a wide range of applications, due to the far greater range of neutrons as compared to charged particle beams (g/cm^2 as compared to 10's of mg/cm^2), together with the fact that isotope production facilities often produce large secondary neutron fields. Particular interest has been paid to (n,p) and (n,α) charge-exchange reactions since these reactions produce high-specific activity radionuclide samples without the use of chemical carriers in the separation process.

Two other potential neutron sources for (n,x) reactions exist in addition to the secondary neutron fields generated at existing isotope production facilities: reactors and neutron generators that utilize the D(T,n)α "DT" and D(D,n)^{3}He "DD" reactions. While reactors produce copious quantities of neutrons, their energy spectrum is often not well-suited to the preparation of high-purity samples due to the co-production of unwanted activities via neutron capture, in addition to the significant start-up costs and proliferation concerns involved in their commissioning. Similarly, while the higher energy 14-15 MeV neutrons produced at DT generators are capable of initiating (n,p) and (n,α) reactions, their higher energy opens the possibility of creating unwanted activities via (n,pxn) and (n,αxn) reactions that cannot easily be separated from the desired radionuclides.

In contrast, while the neutron spectrum from a DD reaction, which ranges from approximately 2-3 MeV, is ideally suited to radionuclide production, the lower flux from these generators limits their production rate. An additional complication is the relative paucity of high-quality, consistent cross section data for neutrons in the 2-3 MeV DD energy range.

The purpose of the present work is to explore the potential for using high-flux neutron generators to make high-specific activity samples of radionuclides at the mCi level for local use in the application community. The research group at UC-Berkeley has been developing a High Flux Neutron Generator (HFNG) that features an internal target where samples can be placed several mm from the neutron producing surface in order to maximize the utilization of each neutron for the production of a desired radionuclide [XXXref Cory paper]. The HFNG uses the D(D,n)^{3}He reaction to produce neutrons with energies near 2.45 MeV together with a self-loading target design to maintain continuous operation without target replacement. In addition to the generator itself, efforts are underway to design neutron reflection capabilities to allow scattered neutrons multiple opportunities to interact with an internally mounted target. While these design efforts are underway, the HFNG can be used to better characterize production cross sections at the appropriate neutron energy.

ASV: cite Cory's paper

The present work features a pair of cross section measurements for the production of two non-standard positron emitters: ^{64}Zn(n,p)^{64}Cu and ^{47}Ti(n,p)^{47}Sc. ^{64}Cu ($t_{1/2}$ = 12.7 h) undergoes β^+ decay (61.5% branching ratio) to ^{64}Ni or β^- decay (38.5% branching ratio) to ^{64}Zn. The emitted 190-keV β^- particle makes this an attractive short-range therapeutic radionuclide, which also has the possibility for simultaneous positron emission tomography (PET) imaging for real-time dose monitoring and verification. This makes ^{64}Cu particularly attractive for emerging radiation therapy protocols. In addition, copper radiochemistry is well developed, and many existing ligands and carriers may be used for selective delivery of the radionuclide to different sites in patients. The second radionuclide studied, ^{47}Sc ($t_{1/2}$ = 3.35 d), undergoes β^- decay to ^{47}Ti, emitting a high-intensity 159-keV gamma ray in the process. This radionuclide is attractive as an emerging diagnostic isotope, due to the similarity of the emitted gamma ray to that of the more well-established ^{99m}Tc. However, due to

the short half-life of and dwindling supplies of ^{99m}Tc, ^{47}Sc stands poised as a potential solution to this shortage, due to its longer half-life and multiple production pathways without the need for highly enriched uranium. In addition, when paired with ^{44}Sc, ^{47}Sc forms a promising "theranostic" set for use in simultaneous therapeutic and diagnostic applications.

ASV: cite theranostic papers, etc

Current methodology in radiochemistry has been proven to successfully recover upwards of 95% of produced ^{64}Cu and ^{47}Sc from solid target designs, without the need for additional carrier. By expanding the base of efficient reaction pathways, great advances can be made in making production of medical radionuclides more efficient and affordable for those in need.

2. Experiment

2.1. Neutron source

ASV: Regex to replace all hard figure references with LaTeX cross-references

Neutron activation was carried out via irradiation in the High-Flux Neutron Generator (HFNG), a DD neutron generator at the University of California, Berkeley. This generator extracts deuterium ions from an RF-heated deuterium plasma through a nozzle, whose shape was designed to form a flat-profile beam 5 mm in diameter. This deuterium beam is incident upon a water-cooled, self-loading titanium-coated copper target, where the titanium layer acts as a reaction surface for DD fusion, producing neutrons with a well-known energy distribution as a function of emission angle [1]. Targets are inserted in the center of the target, approximately 8 mm from the DD reaction surface, prior to startup. Figure 1 displays a cut-away schematic of the HFNG. A 100 kV deuterium beam was extracted at 1.3 mA, creating a flux of approximately $1.3 \cdot 10^7$ neutrons/cm^{2}s on the target.
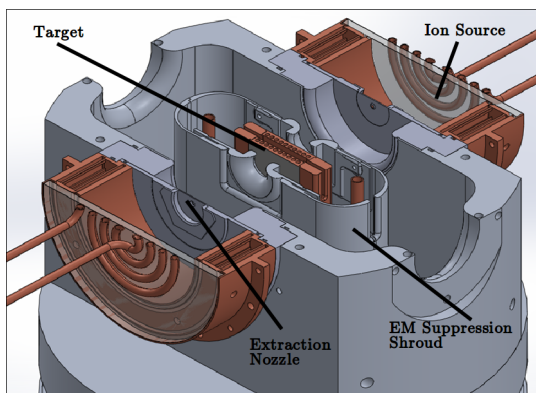

Figure 1. Cut-away schematic of the HFNG. Note: the ion source is approximately 20 cm in diameter.
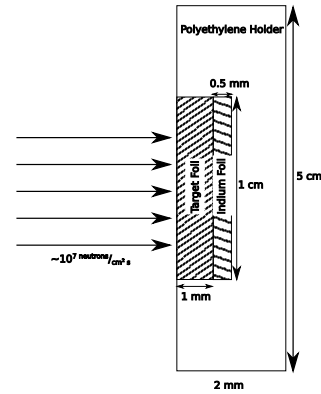

Figure 2. Schematic (not drawn to scale) of the sample holder used for the Berkeley HFNG,

2.2. Cross section determination by relative activation

The approach used in both measurements was to irradiate foils of zinc or titanium, which were co-loaded with indium foils in order to determine their (n,p) cross sections relative to the well-established ^{113}In(n,n')^{113m}In and ^{115}In(n,n')^{115m}In neutron dosimetry standards. Table 1 records physical characteristics of each foil for the various irradiations. In each experiment, the co-loaded foils were irradiated for 3 hours at nominal operating conditions of 1.3 mA and 100 kV. After irradiation, the foils were removed and placed in front of an appropriate High-Purity Germanium gamma-ray detector and the decay gamma-rays were recorded in variable-time bins.

1 cm diameter, 1 mm thick natural abundance zinc and titanium targets were employed for the measurement. Each of these was co-loaded with a natural abundance Indium foil of 1 cm diameter and 0.5 mm thickness in a recess cut into a 2-mm thick polyethylene holder, as seen in Figure 2, which was mounted in the HFNG target center. Prior to loading, each foil was washed with isopropanol and dried, to remove any trace oils or residue that could become activated during irradiation.

ASV: Regex to replace table hard link with LaTeX cross-reference.

ASV: Need foil data from Mauricio's 2nd Ti run

2.3. Determination of effective neutron energy

The D(D,n)^{3}He reaction at 100 keV lab energy produces neutrons with energies ranging from 2.2 to 2.85 MeV, over an angular range of 0-180° in the lab frame-of-reference with respect to the incident deuteron beam. This distribution has been well documented [1] and is shown in Figure 3 for 100 keV incident deuteron energy.

ASV: These 2.2 to 2.85 MeV numbers do not quite correspond to the Figure. Addressing this with Joe.

ASV: Is the one good reference (Liskien) sufficient?

Table 1. Foil characteristics for each of the three (Zn/In)* experiments and the two (Ti/In)† experiments.

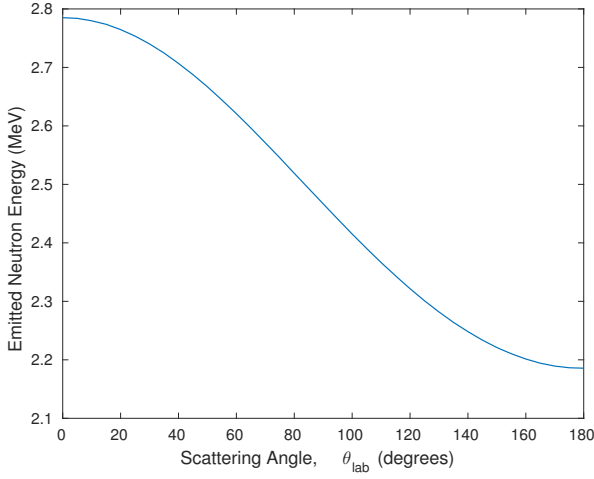| Foils Used	Metal Purity	Abundance (a/o)	Foil Density (mg/cm^2)	Thickness (mm)	Diameter (cm)	Mass (g)
^{nat}In	>99.999%	^{113}In (4.29%), ^{115}In (95.71%)	365.5	0.49 ± 0.02*, 0.50 ± 0.03*, 0.49 ± 0.03*, 0.53 ± 0.06†, XXX $\pm$ XXX†	9.75 ± 0.09*, 9.98 ± 0.15*, 9.96 ± 0.10*, 10.01 ± 0.11†, XXX $\pm$ XXX†	0.248*, 0.248*, 0.241*, 0.247†, XXXXXX†
^{nat}Zn	>99.99%	^{64}Zn (49.17%)	714.1	1.03 ± 0.01, 1.03 ± 0.01, 1.02 ± 0.01	9.93 ± 0.14, 9.76 ± 0.17, 9.89 ± 0.15	0.538, 0.451, 0.452
^{nat}Ti	99.999%	^{47}Ti (7.44%)	450.6	1.16 ± 0.02, XXXXXX	9.93 ± 0.04, XXXXXX	0.337, XXXXXXX

Figure 3. Energy-angle distribution for neutrons emitted following DD fusion, for 100 keV incident deuterons.

Figure 4. MCNP6 model of the HFNG target chamber, with reference scale. The co-loaded foils can be seen in the target chamber center. The ovals indicate the location of water cooling channels.

> ASV: Should we say more about the neutron angular and energy distributions? Something from Cory's thesis or the NIM-A papers that are coming along?

Since the samples are separated by only 8 mm from the DD reaction surface they subtend a fairly significant (28°) angular range and experience an impressive (approximately $1.3 \cdot 10^7$ neutrons/cm^2 s) neutron flux. This stands in contrast to other measurements which feature collimated beams and significantly lower total neutron flux.

> ASV: Need to replace this figure w/ non-capitalized labels - this figure needs significant work, and I would appreciate anyone who can provide a better one

The Monte Carlo N-Particle transport code MCNP6 [2] was used to model the neutron energy spectrum incident upon target foils co-loaded into the HFNG (see Figure 5). This spectrum illustrates the forward-focused kinematics of the DD reaction subtended by the co-loaded sample foils.

While this shows that the sample foils experience a very narrow energy distribution of incident neutrons, an

Figure 5. MCNP6-modeled neutron energy spectrum for the HFNG. The solid lines show the spectrum at the location of the indium and the target foil respectively. The dotted and dashed lines show the same with the target itself "voided" to remove scattering contributions. Less than 1% of the neutrons incident on the foils can be attributed to scatter in the neutron production target.

Figure 6. Fraction of total reactions induced in the Indium foil between the energies [0, E']. The red arrows indicate the energy region that corresponds to 67% of the total activation.

effective neutron energy window must be determined. The MCNP6 simulation shows an identical flux-weighted average neutron energy of 2.765 MeV for both the Indium and target foils to the 1 k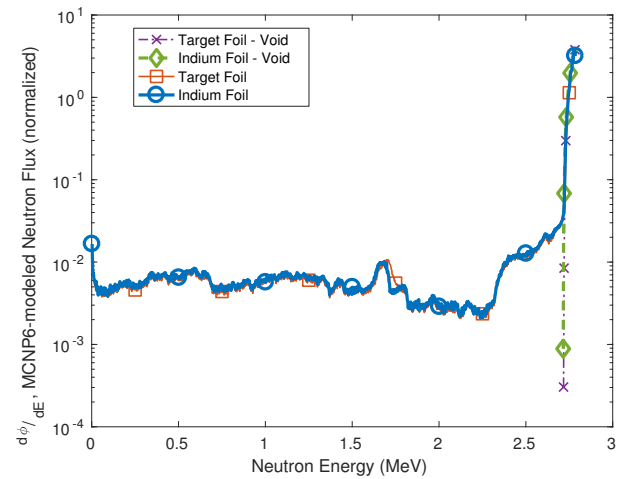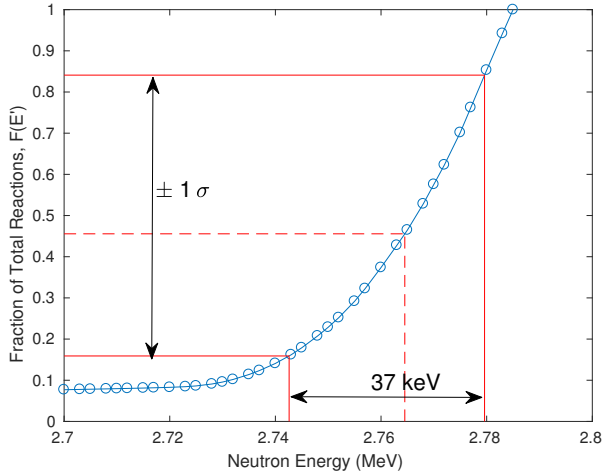eV level. Due to the kinematics of DD neutron emission, E_{max}, the maximum energy of a neutron subtending the target foils in this geometry is 2.783 MeV. For this maximum energy, the number of reactions induced in a foil (containing N_i target nuclei) is given by:

$$R = N_i \int_0^{E_{max}} \sigma(E) \frac{d\phi}{dE} dE \tag{1}$$

> ASV: Regex to replace equations with LaTeX formats, add cross-references.

From this definition, it is possible to calculate $F(E')$, the fraction of total reactions induced up to some energy $E' < E_{max}$:

$$F(E') = \frac{\int_0^{E'} \sigma(E) \frac{d\phi}{dE} dE}{\int_0^{E_{max}} \sigma(E) \frac{d\phi}{dE} dE} \tag{2}$$

> ASV: Change Figure 6 text from the $\pm 1\sigma$ to 68.2%

This quantity $F(E')$ is plotted in Figure 6. The fraction of total reactions in the indium foil can be used to characterize the effective neutron energy bin. Our approach, in analogy to the Gaussian quantity σ, will be to use a horizontal "error bar" to represent the energy range responsible for 68.2% of the reactions taking place. Using this approach, we report the effective energy bin as being $E_n = 2.7645$ MeV + 0.0151 MeV / - 0.0219 MeV. This 37-keV full-energy spread verifies that, at such close distances to the DD reaction surface, loaded target foils receive a quasi-monoenergetic neutron flux.

2.4. Measurement of induced activities

After irradiation, the co-loaded targets were removed from the HFNG and transferred to a counting lab, where their induced activities could be measured via gamma ray spectroscopy. Two detectors were used in this measurement. An Ortec 80% High-Purity Germanium (HPGe) detector was used for the detection of the positron annihilation radiation from the ^{64}Cu decay, the 336 keV gamma-ray from the decay of the ^{115m}In isomer and the 391 keV gamma-ray from the ^{113m}In isomer. An Ortec planar Low-Energy Photon Spectrometer (LEPS) was used for the detection of the lower-energy 159 keV gamma-ray from ^{47}Sc as well as the two indium isomers mentioned above. Both detectors were calibrated for energy and efficiency, using ^{133}Ba, ^{137}Cs, and ^{152}Eu sources at various distances from the front face of each detector. These efficiencies, along with gamma ray intensities for each transition, are used to convert the integrated counts in each gamma ray photopeak into an activity for the activated isotopes and isomeric states.

> ASV: You should add a table listing the gamma-ray properties for the indium isomers and the 64Cu and 47Sc decay lines. This should include the proper NDS citation.

The foils were counted in their polyethylene holder, 10 cm from the front face of the 80% HPGe and 1 cm from the front face of the LEPS, with the target foil (zinc or titanium) facing towards the front face of the detector when both target and monitor foils were counted simultaneously. All data collection was performed using the Ortec MAESTRO software. For each experiment the detector dead time was verified to be less than 5%. No summing corrections need to be made since all of the gammas are either non-coincident or formed in a back-to-back annihilation event. This was never an issue for any experiments, but had it been, the foils would be moved to a position of greater standoff from the detector.

For the ^{47}Sc production experiments, the foils were counted simultaneously using a planar LEPS detector. For the ^{64}Cu production experiments, the Indium foil was first counted separately using an 80% HPGe detector, to capture the short-lived Indium activities. This is due to the fact that the ^{115}In(n,γ) reaction results in the production of ^{116}In which has a 54 minute half-life and results in the production of 1097 keV (58.5% branching), 1293 keV (84.8% branching) and 2112 keV (15.09% branching) gamma-rays that in turn produce a significant number of 511 keV gammas from pair-production followed by annihilation. The foils were counted together again after approximately 4 hours of separate collection, to allow for nearly all of the ^{116}In to decay. Example spectra for each production pathway can be seen in Figure 7a and Figure 7b.

To verify that each peak corresponds to the assigned decay product, spectra were acquired in a sequence of 15 - 30 minute intervals. The resulting time series displayed in Figures 8a - 8d allow the fitting of exponential decay functions for each nuclide and comparison of the measured
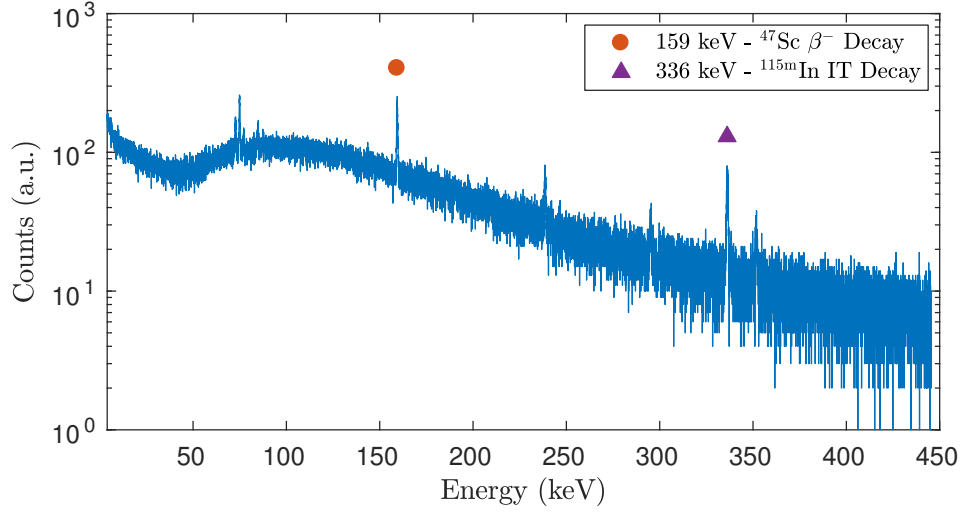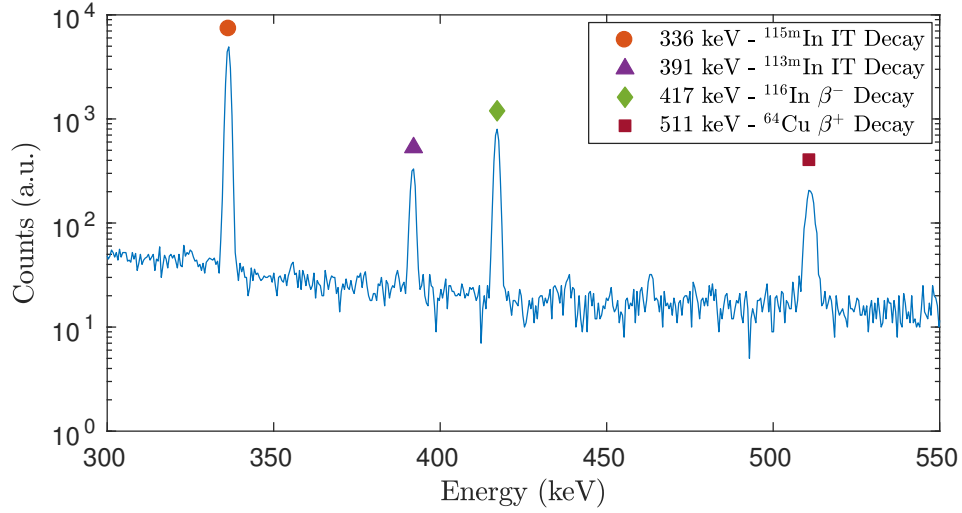
(a) Gamma spectrum for the ^{47}Ti(n,p)^{47}Sc production pathway foils, counted using a LEPS detector

(b) Gamma spectrum for the ^{64}Zn(n,p)^{64}Cu production pathway foils, counted using an 80% HPGe detector.

Figure 7. Example gamma spectra collected to monitor radioisotope production.

half-life with literature values. The fitted functions for each transition agree (at the 1σ confidence level) with accepted half-lives [XXXref reference original papers for the T1/2s], confirming the respective peak assignments.

> ASV: Reference original ENSDF papers

The spectra for the different samples were summed and the peak area over background was determined using gf3, part of the RadWare analysis package from Oak Ridge [3, 4]. The background-subtracted integrated counts in each photopeak, as well as the counting duration for each experiment, are tabulated in Table 2.

2.5. Experimental verification of incident neutron energy

As shown in subsection 2.2 above, the effective neutron energy depends on the angle range subtended by the sample with respect to the incident deuteron beam. In order to determine this angle it is necessary to measure the lateral location of the beam with respect to the sample location.

This centroid of the beam was measured using a 3 x 3 array of 0.5 cm diameter indium foils. The relative activity of these foils was then determined via post-irradiation counting of the ^{115m}In isomer ($t_{1/2} = 4.486$ h). **??** below shows the measured activities for these 9 indium foils. Based on these values we are able to verify that the beam was indeed centered on the middle of the zinc and titanium samples.

> ASV: cire relevant NDS article for t1/2

> ASV: CHECK WITH ERIC for 3x3 In info and plot

2.6. Calculation of measured cross sections

For a thin target consisting of N_T target nuclei (with a reaction cross section $\sigma\left(\bar{E}\right)$), subjected to a constant neutron flux $\phi\left(\bar{E}\right)$, the rate of production (R) of the product nucleus will be:

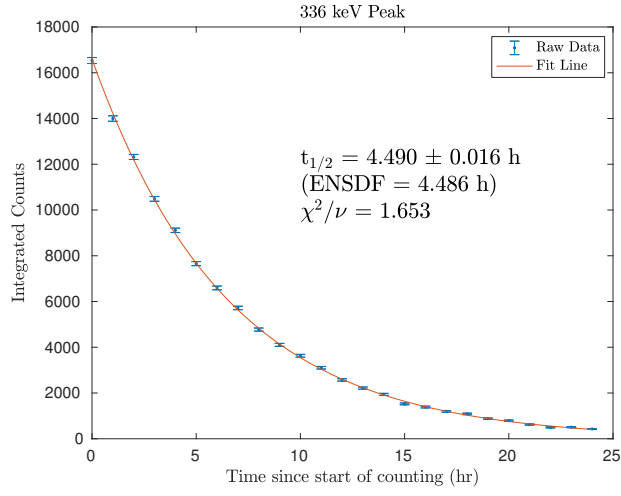$$R = N_T \sigma\left(\bar{E}\right) \phi\left(\bar{E}\right) \tag{3}$$
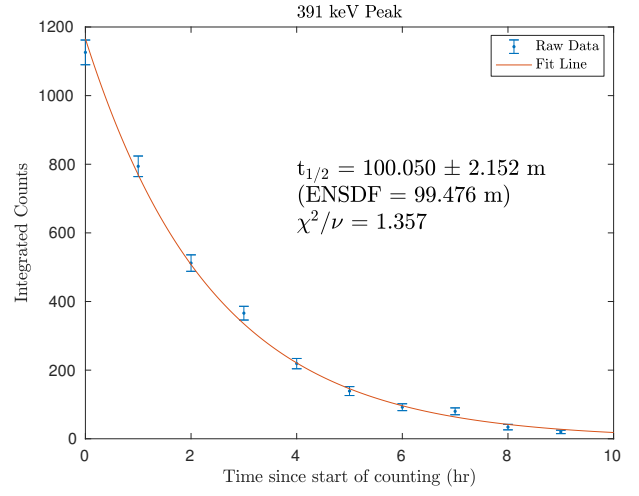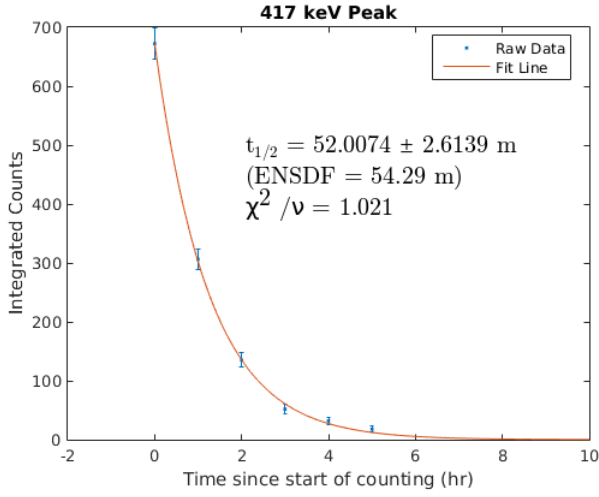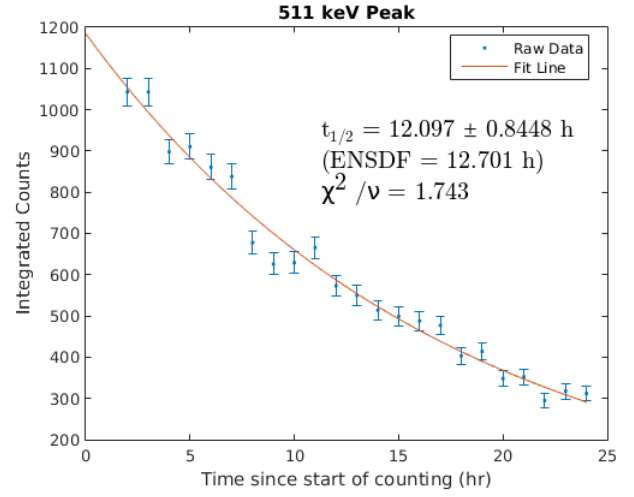
(a) Decay curve for the isomeric transition of ^{115m}In.

(b) Decay curve for the isomeric transition of ^{113m}In.

(c) Decay curve for the β^- decay of ^{116}In.

(d) Decay curve for the β^+ decay of ^{64}Cu.

Figure 8. Decay curves used to verify photopeak transition assignment.

Table 2. Counting times and photopeak counts for each of the (Zn/In) and (Ti/In) experiments. Need Mauricio data!

Reference Foil	^{nat}In	^{nat}In	^{nat}In	^{nat}In	^{nat}In
Reference Foil Mass (g)	0.248	0.248	0.241	0.247	XXXXXX
Target Foil	^{nat}Zn	^{nat}Zn	^{nat}Zn	^{nat}Ti	^{nat}Ti
Target Foil Mass (g)	0.538	0.451	0.452	0.337	XXXX
Irradiation Time, t_1 (s)	10800	10800	12629	11837	XXXX
Start of Count, t_2 (s)	12585	26985	14919	101245	XXXX
End of Count, t_3 (s)	103773	80993	68919	187669	XXXX
Photopeak Counts, 336 keV (^{115m}In)	113665 ± 1490	74321 ± 275	XXXXX	2122 ± 55	XXXX
Photopeak Counts, 391 keV (^{113m}In)	3382 ± 171	860 ± 40	XXXXX	————	————
Photopeak Counts, 511 keV (^{64}Cu)	16055 ± 643	12852 ± 118	XXXXX	————	————
Photopeak Counts, 159 keV (^{47}Sc)	————	————	————	3877 ± 83	XXXX

If this irradiation lasts for some time t_1, and gamma ray spectrum acquisition begins at a later time t_2 and ends at t_3, then the number of product decays (D; with decay constant λ) during the acquisition will be:

$$D = \frac{R}{\lambda} \left(e^{\lambda t_1} - 1\right) \left(e^{-\lambda t_3} - e^{-\lambda t_2}\right)$$
$$= \frac{N_T \sigma\left(\bar{E}\right) \phi\left(\bar{E}\right)}{\lambda} \left(e^{\lambda t_1} - 1\right) \left(e^{-\lambda t_3} - e^{-\lambda t_2}\right) \quad (4)$$

If this decay emits a gamma ray with branching ratio I_γ (photons emitted per decay), and is detected with an absolute efficiency of ϵ_γ (photons detected / photons emitted), then the number of observed decays between t_2 and t_3 will be:

$$N_{obs} = D\epsilon_\gamma I_\gamma \quad (5)$$
$$= \epsilon_\gamma I_\gamma \frac{N_T \sigma\left(\bar{E}\right) \phi\left(\bar{E}\right)}{\lambda} \left(e^{\lambda t_1} - 1\right) \left(e^{-\lambda t_3} - e^{-\lambda t_2}\right)$$

Solving this equation for the cross-section results in:

$$\sigma\left(\bar{E}\right) = \frac{N_{obs}\lambda}{N_T \epsilon_\gamma I_\gamma \phi\left(\bar{E}\right) \left(e^{\lambda t_1} - 1\right) \left(e^{-\lambda t_3} - e^{-\lambda t_2}\right)} \quad (6)$$

Equation 6 can be used to determine the unknown (n,p) cross sections relative to the well-known ^{115}In(n,n')^{115m}In and ^{113}In(n,n')^{113m}In inelastic scattering cross sections since the Zn and Ti samples were co-irradiated with indium foils. This approach has a number of advantages since the result is independent of neutron flux and only depends on the relative detector efficiencies at each gamma-ray energy. Equation 7 shows the ratio of the cross sections determined using this approach, in which subscript P indicates a quantity for either ^{64}Cu or ^{47}Sc, and subscript In indicates a quantity for either the ^{113m}In or ^{115m}In isomer. A minor term was added to correct for the small self-attenuation of the gamma rays emitted by the activated foils:

$$\frac{\sigma_P}{\sigma_{In}} = \frac{A_P}{A_{In}} \frac{N_{T,In}}{N_{T,P}} \frac{\lambda_P}{\lambda_{In}} \frac{e^{\lambda_{In} t_1} - 1}{e^{\lambda_P t_1} - 1} \quad (7)$$
$$\times \frac{e^{-\lambda_{In} t_3} - e^{-\lambda_{In} t_2}}{e^{-\lambda_P t_3} - e^{-\lambda_P t_2}} \frac{\epsilon_{In}}{\epsilon_P} \frac{I_{\gamma,In}}{I_{\gamma,P}} \frac{e^{-\mu_{In} x_{In}/2} \times e^{-\mu_{In} x_P}}{e^{-\mu_P x_P/2}}$$

where:

- A is the integrated counts under a photopeak [counts],

- σ is the cross section for either the production of a product or isomer [mb],

- N_T is the initial number of target nuclei,

- λ is the decay constant [s^{-1}],

- t_1 is the irradiation time [s],

- t_2 is the time between the start-of-beam and the start of counting [s],

- t_3 is the time between the start-of-beam and the end of counting [s],

- ϵ is the detector efficiency for a particular photopeak,

- I_γ is the decay gamma ray branching ratio,

- μ is the photon attenuation coefficient for a particular decay gamma ray in a foil [cm^{-1}],

- and x is the thickness of foil traversed by a particular decay gamma ray [cm]

In addition to the ^{115}In(n,n')^{115m}In reference cross section, the ^{115}In(n,γ)^{116m}In ($t_{1/2} = 54.29$ min) activity can be used to determine the ^{64}Zn(n,p) and ^{47}Ti(n,p) cross section. The capture activity is potentially subject to contamination from lower energy, especially thermal, "room return" neutrons since the (n,γ) cross section at 25 meV is approximately YYY MeV greater than at 2.7 MeV.

ASV: cite relevant NDS article

ASV: add appropriate numbers to (n,g) cross sections

ASV: cite IRDFF somewhere?

With the exception of decay constants, which have negligible uncertainty compared to other sources of uncertainties in this work, each of the parameters in this model carries a statistical uncertainty. Based on the assumption that these uncertainties are independent, the total relative statistical uncertainty δ_σ is calculated by taking the quadrature sum of the relative uncertainties of each parameter δ_i:

$$\delta_\sigma = \|\vec{\delta}\|_2 = \sqrt{\sum_{i=1}^{N} \delta_i^2} \quad (8)$$

This total statistical uncertainty will be plotted as the cross-section error bar in the excitation function for these production reactions.

2.7. Systematic errors

The largest source of systematic uncertainty in the cross section determined via the "ratio approach" is the YYY% uncertainty in the ^{115}In(n,n')^{115m}In cross section and the YYY% uncertainty in the ^{113}In(n,n')^{113m}In cross section. An additional uncertainty arises from the fact that the Zn/Ti samples are not located at exactly the same location as the indium monitor foils, and are therefore not subject to precisely the same neutron flux. However, the MCNP6 simulations shown in Figure 5 indicate that the difference in the flux that the two foils are subjected to is less than YY%. Other monitor foils could be used instead of indium, with ^{57}Ni(n,p)^{57}Co being one possible candidate, but the 4.486 hour and 99.476 minute half-lives of the ^{115m}In and ^{113m}In isomers [XXXref NDS], respectively, makes indium a better candidate for measuring the production of radionuclides with lifetimes much less than 77+ days. The largest source of uncertainty in energy window arises from uncertainties in the actual dimension of the deuteron beam on

the production target. We believe, based on "burn marks" on the production target that the beam was approximately circular, with a flat intensity profile and a 5 mm diameter. However, every 1 mm change in the beam radius would cause a XXX MeV shift in the centroid and a YYY MeV change in the effective energy bin.

> ASV: filling in missing data

> ASV: Use your energy-angle figure from Lisken above to estimate these numbers. You can point to the figure in the text if you'd like.

3. Results

Using the ratio method described here, the cross sections for the ^{47}Ti(n,p)^{47}Sc and ^{64}Zn(n,p)^{64}Cu reactions have been calculated for incident neutron energy of 2.7645 MeV, + 0.0151 MeV / - 0.0219 MeV. These values are recorded in Table 3.

> ASV: Need Mauricio's Cu point w/ more sigfigs. Need Mauricio's Sc point too

> ASV: Truncate sig figs here - Note that the systematic uncertainty you calculated in the previous paragraph will provide a natural limit on the number of significant figures you quote for the energy window.

> ASV: Report a weighted average between the solo values, insert in text

> ASV: Truncate sig figs in En in Table 3

The results for the ^{47}Ti(n,p)^{47}Sc and ^{64}Zn(n,p)^{64}Cu production cross sections can also be seen plotted in Figures 9 and 10, respectively. It is apparent that the relative cross sections measured in the present work are consistent with both the small quantity of other literature results, and are measured to within 6% uncertainty, lower than existing measurements. In addition, the results presented in this work show strong agreement with the recommended values from both the ENDF/B-VII.1 nuclear data library and reaction modeling results from TALYS[5].

Table 3. Results of cross section measurement. Note that the last data point for the ^{47}Sc measurement (marked with *) was performed at a slightly different beam spot location, leading to a difference in effective neutron energy.

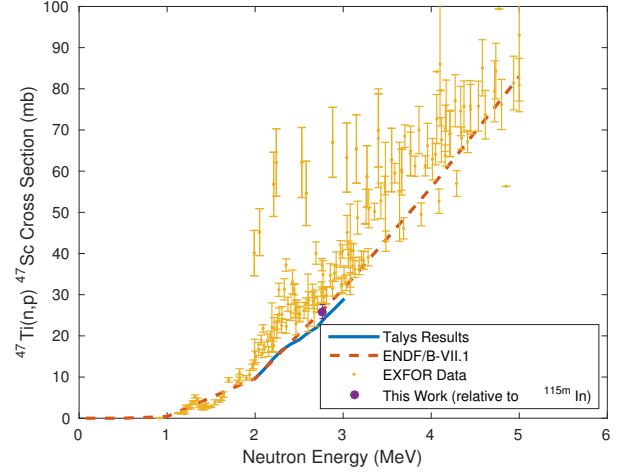| Reaction	$\sigma(E_n = 2.7645$ MeV) (mb)
^{64}Zn(n,p)^{64}Cu (relative to ^{113}In)	45.953 ± 3.351, 46.493 ± 2.805, 46.9 ± 3.189
^{64}Zn(n,p)^{64}Cu (relative to ^{115}In)	49.716 ± 3.335, 49.011 ± 2.698, XXXX ± XXXXXX
^{47}Ti(n,p)^{47}Sc (relative to ^{115}In)	25.901 ± 1.7089, XXXXX ± XXXXX

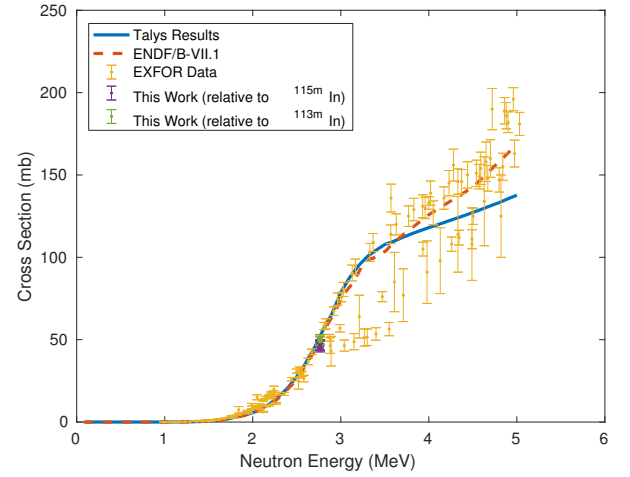Figure 9. Measured ^{47}Ti(n,p)^{47}Sc relative production cross section.

Figure 10. Measured ^{64}Zn(n,p)^{64}Cu relative production cross section

> ASV: Waiting on Lee for EMPIRE, ALICE data and language discussing differences and the significance of this.

> ASV: Mention Shimizu data specifically?
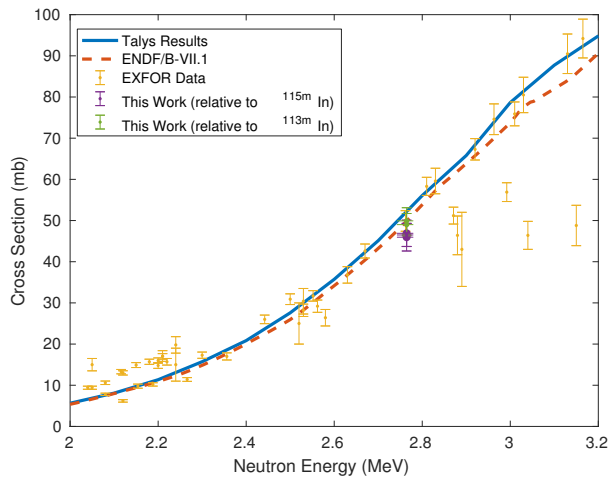
> ASV: Add a zoomed-in view like in Figure 10?

Figure 11. A zoomed-in view of Figure 10.

4. Summary

Using direct activation methods for thin foils as described in this work, the ^{47}Ti(n,p)^{47}Sc and ^{64}Zn(n,p)^{64}Cu production cross sections have been measured for 2.7645 MeV neutrons, to within 6% uncertainty. These measurements are consistent with experimental data and theoretical models, and have been measured to lower uncertainty than existing measurements. The use of DD neutron generators can be an efficient pathway for the measurement of these low-energy (n,p) reaction channels, as well as a relative method used to normalize measurements at higher neutron energies. While it reduces the neutron flux incident upon target foils, the use of collimated beam lines to irradiate foils at various angles allows a single neutron generator to perform these measurements at various other energies throughout the DD neutron emission energy spectrum.

> ASV: Future work? Thermal neutron measurements? Something like the following?

Future work will involve the continued measurement of the (n,p) production cross sections for various other emerging therapeutic and diagnostic radioisotopes, to expand the toolset of options available for modern medical imaging and cancer therapy. This will focus on radionuclides which permit more customized and precise dose deposition, as well as patient-specific treatments

> ASV: Should we specifically mention other isotopes we plan to measure?

5. Acknowledgements

> ASV: Who else should we acknowledge?

References

[1] H. Liskien and A. Paulsen, "Neutron production cross sections and energies for the reactions T(p,n)3He, D(d,n)3He, and T(d,n)4He," *Atomic Data and Nuclear Data Tables*, vol. 11, no. 7, pp. 569–619, 1973.

[2] J. T. Goorley, M. R. James, T. E. Booth, F. B. Brown, J. S. Bull, L. J. Cox, J. W. J. Durkee, J. S. Elson, M. L. Fensin, R. A. I. Forster, J. S. Hendricks, H. G. I. Hughes, R. C. Johns, B. C. Kiedrowski, R. L. Martz, S. G. Mashnik, G. W. McKinney, D. B. Pelowitz, R. E. Prael, J. E. Sweezy, L. S. Waters, T. Wilcox, and A. J. Zukaitis, "Initial MCNP6 release Overview - MCNP6 version 1.0," *LA-UR-13-22934*, 2013.

[3] D. C. Radford, "Notes on the use of the program gf3," 2000.

[4] D. C. Radford, "ESCL8R and LEVIT8R: Software for interactive graphical analysis of HPGe coincidence data sets," *Nuclear Inst. and Methods in Physics Research, A*, vol. 361, pp. 297–305, jul 1995.

[5] A. J. Koning, S. Hilaire, and M. C. Duijvestijn, "TALYS: Comprehensive nuclear reaction modeling," in *AIP Conference Proceedings*, vol. 769, pp. 1154–1159, IOP INSTITUTE OF PHYSICS PUBLISHING LTD, 2005.

H. F. Aly et al., Microchim. Acta, vol. 59, no. 1, 1971.

K. S. Bhatki et al., J. Radioanal. Chem., vol. 2, no. 1-2, 1969.

T. H. Bokhari et al., J. Radioanal. Nucl. Chem., vol. 283, no. 2, 2010.

J. F. Briesmeister et al., Los Alamos National Laboratory, 1986.

M. B. Chadwick,et al., Nucl. Data Sheets, vol. 107, no. 12, 2006.

A. J. Koning et al., AIP Conference Proceedings, 2005, vol. 769, no. 2.

H. Liskien et al., Nucl. Data Tables, vol 11, 1973.

M. R. Lewis et al., J. Nucl. Med., vol. 44, no. 8, Aug. 2003.

C. MÃijller et al., J. Nucl. Med., vol. 55, no. 10, Oct. 2014.

N. Otuka et al., Nucl. Data Sheets, vol. 120, 2014.

L. Pietrelli et al., J. Radioanal. Nucl. Chem., vol. 157, no. 2, 1992.

S. M. Qaim et al., IAEA Technical Reports Series No. 473, 2011.

T. Shimizu, et al, Ann. Nucl. Energy, vol. 31, no. 9, pp. 975-990, 2004.

T. Shimizu, et al, Nucl. Instruments Methods Phys. Res. Sect. A Accel. Spectrometers, Detect. Assoc. Equip., vol. 527, no. 3, pp. 543-553, 2004.

D. Updegraff et al., "Nuclear Medicine without Nuclear Reactors or Uranium Enrichment," 2013.

> ASV: Cite Cory's thesis, or upcoming NIM paper?

> ASV: Convert these to BibTeX format!